

Numerical Simulation of Parametric Roll in Head Seas

Dimitris Spanos, *National Technical University of Athens*

Apostolos Papanikolaou, *Ship Design Laboratory (NTUA-SDL)*

ABSTRACT

A time-domain numerical simulation method is applied for the investigation of parametric roll resonance in regular head waves for two different types of vessels, namely a fishing vessel and a RoRo ship. The employed mathematical model captures satisfactorily most of the parameters relevant to the problem hence enables an improved reproduction and understanding of the complicated non-linear parametric roll phenomenon. The coupling between the induced roll and pitch motions along with the nonlinear character of the restoring moment associated with large amplitude wave induced motions have been found to be the determinant factors of the observed roll resonance phenomenon. Furthermore, a strong dependence of the roll resonance on both the wave frequency of encounter and the incident wave height has been recorded. The obtained numerical results were compared with corresponding available experimental measurements and commented.

Keywords: *time-domain, numerical simulation, parametric resonance, roll motion, non-linear dynamics, dynamic stability, capsizing*

1. INTRODUCTION

The phenomenon of parametric roll has been extensively studied over the last decades, but it still remains of high interest because of the practical implications related to the induced large amplitude roll motions (e.g., France et al. 2003) and due to its complicated highly non-linear character that makes its prediction quite difficult in actual seaways.

Parametric roll is considered as the induced roll motion of a ship due to the periodic change of the restoring characteristics as the ship advances through the waves. Parametric roll is expected to occur when the wave frequency of encounter is close to the double of the natural roll frequency of the vessel. Given this condition, the other parameters of the problem eventually determine the occurrence as well as the intensity of the phenomenon. These parameters are particularly the hull form and the related hydrostatic characteristics, the vessel's loading condition and forward speed,

the roll damping effects and the wave characteristics like wave heights and frequencies.

Several approaches have been employed to analyze and understand the parametric roll phenomenon ranging from the uncoupled, one degree of freedom non-linear roll equation, adjusted with appropriate parameters, e.g. Francescutto (2002), Umeda et al. (2003), to models of multi degrees of freedom, where the roll motion is appropriately coupled with the other motions, Belenky (2003), Ribeiro et al. (2005), Neves, (2005), Krueger (2006). Parametric roll has been investigated for both regular and irregular seaways, as well as for following and head seas conditions. Despite the substantial progress for the regular waves, the resonance conditions in irregular waves have not yet been resolved. A recent review of the related literature has been carried out by ITTC (2005).

In subsequent sections, a nonlinear time-domain numerical simulation method is applied to investigate the behaviour of two different

types of vessels, namely a fishing vessel and a RoRo ship, with respect to parametric rolling in regular head waves. The same method has been applied earlier (Spanos & Papanikolaou, 2005) to systematically explore the physical parameter space of parametric rolling for the fishing vessel. There, a strong nonlinear dependence of the induced roll motion on the incoming wave heights has been observed. In the present paper this behaviour is further analyzed and interpreted in more depth in terms of motion couplings and nonlinear restoring. Having understood and verified numerically the performance of the fishing vessel, a different type of vessel, namely a modern RoRo, is herein additionally studied aiming at exploring the earlier identified basic characteristics of the nonlinear parametric roll phenomenon for a different type of hull form.

2. THE NUMERICAL SIMULATION METHOD

The numerical simulation method applied herein for the evaluation of extreme motions of ships in seaways is a nonlinear time domain numerical method which is based on linear potential theory with respect to the basic hydrodynamics of the problem and considers a variety of important non-linear terms of ship's equations of motions, like the excitation by large amplitude regular or irregular waves, the exact body geometry below and above the still waterline and its impact on ship's restoring, semiempirical nonlinear viscous damping, as well as possible sloshing effects due to moving fluids internally to the vessel or trapped on the deck, (Spanos, 2002).

The mathematical modelling of the method is herein implemented with the computer code CAPSIM. The method has been successfully applied in the past for the simulation of ship motions at zero forward speed in intact and damaged/flooded conditions as well as for the estimation of wave loads and particularly of drift forces on floating bodies, (Spanos & Papanikolaou, 2005b), and proved very

efficient and satisfactory in many practical cases.

The essential characteristics of the method are outlined in the following. The sailing ship is considered rigid and of arbitrary shape moving with six degrees of freedom in response to incident waves. The equations of motion of the body in the 3D space are derived by application of the momentum conservation theorem. The equations are expressed in the ship-fixed coordinated system and are given below

$$m(\dot{\vec{U}} + \vec{\omega} \wedge \vec{U}) = \vec{F} \quad (1)$$

$$[I]\dot{\vec{\omega}} + \vec{\omega} \wedge [I]\vec{\omega} = \vec{M} \quad (2)$$

where m and $[I]$ are the mass and the matrix of moments of inertia of the ship respectively, U and ω the linear and angular velocity and F, M are the external to the ship forces and moments. The velocity U is the relative velocity of the origin of the ship-fixed system to an inertia coordinate system that moves with a constant speed and course.

The external forces acting to the body comprise of gravity, hydrostatic and hydrodynamic components; others might be added in a straightforward way (wind & current forces, etc). Following the potential theory, the wave effects, as the dominant dynamic part, are further analyzed into Froude-Krylov or undisturbed incident wave, diffraction and radiation effects.

Incident wave forces together with the hydrostatic ones are calculated through direct integration of the dynamic and hydrostatic pressure over the instantaneous wetted part of the hull $S_w(t)$, which is defined by the undisturbed incoming wave and the instant position of the ship.

$$\vec{F}_1(t) = \iint_{S_w(t)} p \vec{n} ds \quad (3)$$

where \vec{n} is the unit normal vector and the pressure p comprises both hydrostatic and dynamic terms, according to Bernoulli's potential theory formula.

$$p = -\rho g z - \rho \frac{\partial \Phi}{\partial t} - \frac{1}{2} \rho |\nabla \Phi|^2 \quad (4)$$

where Φ is the velocity potential, ρ the water mass density, g the gravity acceleration, and z the vertical coordinate directing upwards.

The radiation forces are herein calculated by use of the added mass and damping coefficients calculated in the frequency domain and properly transformed into the time domain by application of the impulse response function concept introduced by Cummins (1962).

$$F_{R,i}(t) = -A_{ij}(\infty) \dot{U}_j - \int_0^{\infty} K_{ij}(\tau) U_j(t-\tau) d\tau \quad (5)$$

where $i, j=1 \div 6$, A_{ij} are the added masses at infinite frequency of oscillation and the kernel functions K_{ij} are the impulse response functions corresponding to the damping coefficients calculated in the frequency domain.

For irregular seaway excitation, the elementary diffraction forces, corresponding to the constituent wave frequencies of an assumed irregular sea spectrum, are taken directly proportional to the corresponding elementary diffraction forces calculated in the frequency domain.

Radiation (thus added-masses and damping coefficients) and diffraction forces in the frequency domain were herein calculated by application of the computer code NEWDRIFT, (Papanikolaou, 1989). This is a six-degrees of freedom (6 d.o.f.), three-dimensional (3D) panel code program for the calculation of motions and wave induced loads, including drift force effects acting on arbitrarily shaped bodies in regular waves. The code is based on the zero-speed Green function, pulsating source distribution method and accounts for the forward speed effects considering the slender body theory assumptions. The code employs triangular or quadrilateral panels for the modelling of the wetted ship surface.

Roll viscous effects are taken into account for the roll motion using a semi-empirical linear or quadratic roll velocity model.

The above formulated mathematical model for the present ship-wave (hydro-mechanical) system comprises of a set of six second-order nonlinear differential equations. Integrating this set of equations by a time integration method, the six degrees of freedom motions of the body are obtained in the time domain. Details of the simulation model can be found in (Spanos, 2002).

3. THE NUMERICAL EXPERIMENTS

The herein investigated vessels are, a fishing boat with a transom stern arrangement, and a single screw RoRo vessel with transom stern tunnelled stern sections and a bulbous bow. Despite the fundamental differences of the two hull forms they dispose some common features with respect to their waterplane area, likely to induce the parametric roll phenomenon under certain conditions: due to the intense change of their hull lines around the still waterline, particularly in the stern area, the hydrostatics of both hulls are sensitive to draught and pitch changes.

The details of the studied fishing vessel have been taken from Neves et al. (2002), who have tested the parametric roll of this ship in head waves in model tank. Its main particulars are listed in Table 1 and the geometric model developed for the present study in Figure 1.

Table 1 Main particulars of the fishing vessel

Length (m)	25.91
Length pp (m)	22.09
Beam (m)	6.86
Depth (m)	3.35
Draught (m)	2.48
Displacement (tons)	170.30
Roll radius of gyration (m)	2.215
Pitch radius of gyration (m)	5.522

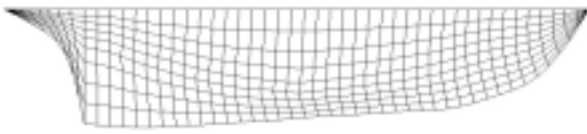


Figure 1 Modeling of wetted surface up to still water for the fishing vessel (2x365 panels)

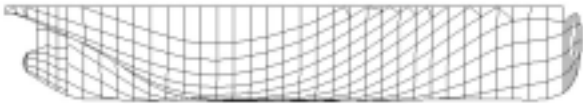


Figure 2 Modeling of the wetted surface up to still water for the RoRo ship (2x438 panels)

The hull characteristics and details of the studied RoRo ship have been disposed to the authors by the German shipyard, Flensburger Schiffbau Gesellschaft (FSG). The main particulars are presented in

Table 2 and the geometric model employed in numerical simulation in Figure 2 below. The radii of gyration assumed herein corresponding to $i_{xx} = 0.325B$ and $i_{yy} = 0.25L$.

Table 2 Main particulars of the RoRo ship

Length pp (m)	190.30
Beam (m)	26.50
Depth (m)	13.25
Draught (m)	7.65
Displacement (tons)	22341.6
Roll radius of gyration (m)	8.613
Pitch radius of gyration (m)	47.573

In the numerical simulation the vessels were free to move in heave, roll and pitch, whereas they were constrained in the other degrees of freedom. These captive numerical tests differ to a certain degree from the corresponding experimental tests in model tank for the fishing vessel, where the model was equipped with two towing lines at the bow and stern respectively as course keeping devices.

This arrangement permits some freedom to sway and yaw motions hence some effects of this on experimental measurements could be present.

In absence of refined roll damping data, the viscous roll damping was herein approximated with a linear model having a damping parameter varying as percentage of the critical roll damping. In Figure 3 the free roll decay of the fishing vessel for two values of damping at zero speed are depicted.

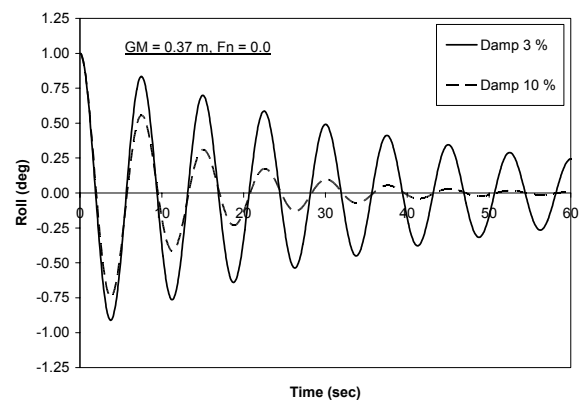


Figure 3 Free roll decay of the fishing vessel

4. SIMULATION RESULTS

The two vessels were tested in conditions of parametric roll resonance in head waves, namely for all the numerical tests the wave frequency of encounter was double the natural roll frequency of the vessel. Systematic variation of the basic parameters that of the vertical centre of gravity KG (correspondingly of the GM), forward speed, roll viscous damping and wave height was performed in order to investigate their effect on the vessels' motion.

The amplitude of the roll motion of the vessels as a function of the wave amplitude or wave height (double wave amplitude) was recorded and is presented in the followings. The recorded roll amplitude corresponds to the steady state response namely when the transients have died out.

The next Figure 4 samples two simulated cases for the studied fishing vessel, with different initial angles, where the steady state response is apparent after a time of 120 seconds. Numerical simulation tests proved that the steady state response was independent of the initial conditions. The next Figure 5 depicts the corresponding time series of the associated pitch motion. It shows that the pitch motion oscillates with the wave frequency of encounter and reaches quite a steady state within the first 20 sec after the start of the simulation.

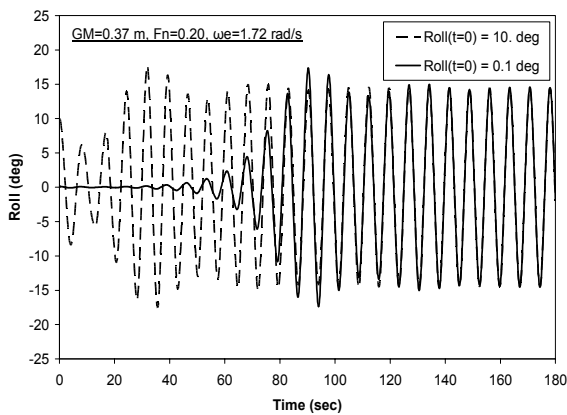


Figure 4 Simulated roll time series

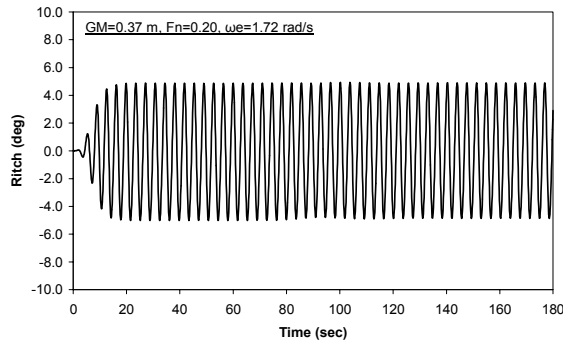


Figure 5 Simulated pitch time series

Figure 6 shows the roll-pitch diagram of the above example. The minimum pitch values (corresponding to trim by stern) occur at the higher roll angles, whereas for intermediate roll angles the maximum pitch (trim by bow) is observed.

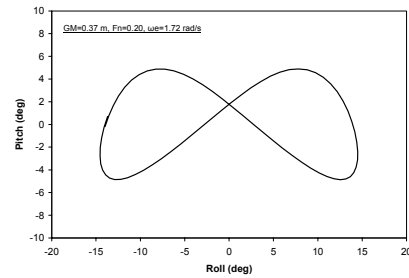


Figure 6 Roll-Pitch diagram

4.1 Fishing Vessel

Figure 7 to Figure 10 present the roll responses for the fishing vessel for two GM values (0.37 m and 0.50 m) and two Froude numbers F_n (0.20 and 0.30). Each curve in the diagrams corresponds to different assumed roll damping.

According to these results the parametric roll starts occurring for wave amplitudes greater than 0.20 m. Thereafter, roll motion increases with the wave amplitude in a complicated way. For the lower GM ($= 0.37$ m) capsizing occurs at wave amplitudes around 0.90 m and 0.70 m for F_n equal to 0.20 and 0.30 respectively. For the higher GM, despite the steeper increase of roll for the lower wave amplitudes, the vessel comes to finite maximum roll amplitude without capsize. For even higher wave amplitudes, greater than those for which the maximum roll occurs, the roll motion amplitude gradually decreases until it diminishes completely.

These numerical results are plotted together with experimental measurements carried out in model tank by Neves et al., (2002). The tank measurements indicate that the numerical simulation captures the onset of the roll resonance, especially for the lower GM value ($= 0.37$ m). In the other case (GM = 0.50 m), there is only single experimental measurements for the higher wave amplitude ($= 1.0$ m) that resulted to zero roll amplitude. The numerical simulation indicates here also the absence of a rolling behaviour for the higher damping ($= 15\%$) whereas for the other damping values

non-rolling is observed at the range of even greater wave amplitudes. This very interesting nonlinear phenomenon, namely the reduction of roll amplitude at the region of larger waves, has also been recorded by Hashimoto et al., (2005) in similar experiments with a container ship in regular head waves. This behaviour has been also identified earlier in a basic theoretical nonlinear model of Umeda et al., (2003). Also, recent experimental measurements for a containership, carried out by Lee et. al. (2006), identify the same behavior, while green water on deck has been regarded as a possible explanatory reason at least for the range of the higher wave heights. In any case, such response needs further detailed investigation in order to clearly identify the causing conditions.

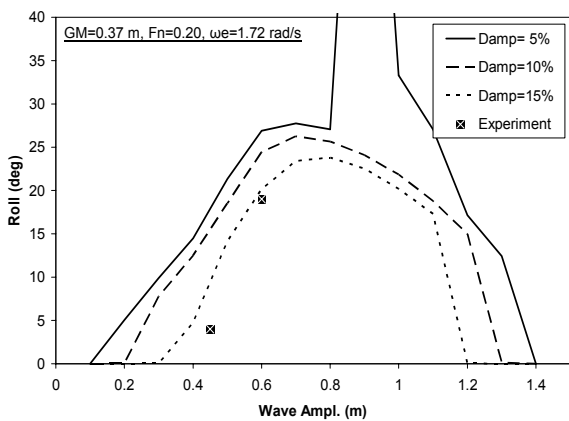


Figure 7 Roll vs. wave height for fishing vessel at $GM=0.37$ and $Fn=0.20$

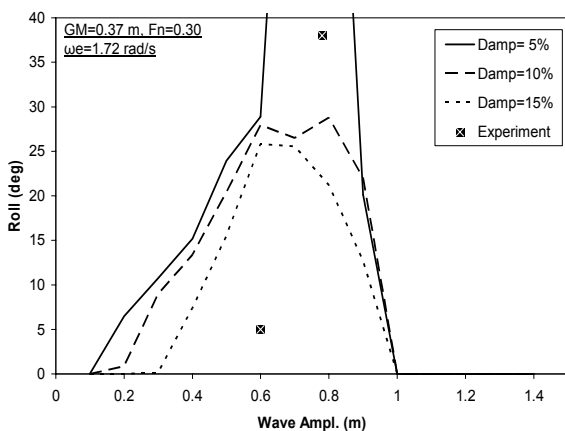


Figure 8 Roll vs. wave height for fishing vessel at $GM=0.37$ and $Fn=0.30$

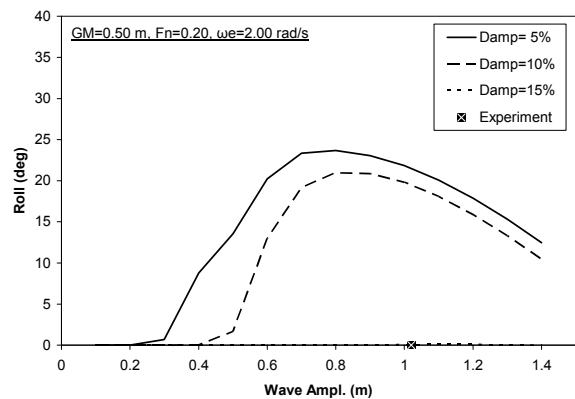


Figure 9 Roll vs. wave height for fishing vessel at $GM=0.50$ and $Fn=0.20$

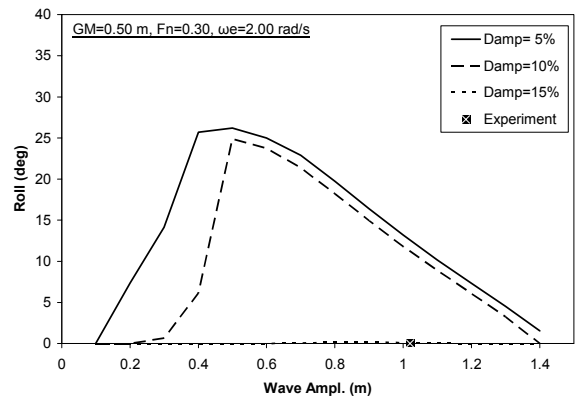


Figure 10 Roll vs. wave height for fishing vessel at $GM=0.50$ and $Fn=0.30$

The effect of viscous damping on the performance of the vessel is always to decrease the induced roll motion. In case of the higher GM value ($= 0.50$ m), a higher viscous damping seems sufficient to cancel the onset of the roll resonance throughout the range of investigated waves.

At the lower wave amplitudes range, up to the maximum roll occurrence, it is interesting to note that in the case of higher GM ($= 0.50$ m) the roll is strongly affected by the vessel's forward speed. In this region, the roll is getting larger with the increase of the speed. In the other case ($GM = 0.37$ m), there is not any notable effect of the forward speed on the roll motion.

4.2 RoRo Vessel

Figure 11 to Figure 14 present the simulated roll motion for the RoRo ship for two GM values (1.00 m and 1.50 m) and for two Froude numbers (0.15 and 0.25). Regular wave heights up to 6 m were investigated.

Roll resonance is observed for the RoRo ship in three out the four presented cases for wave heights greater than 4.0 m. In the case of the lower GM (= 1.00 m) and the higher Fn (= 0.25) no resonance occurred for any of the tested conditions, resulting a zero amplitude roll motion.

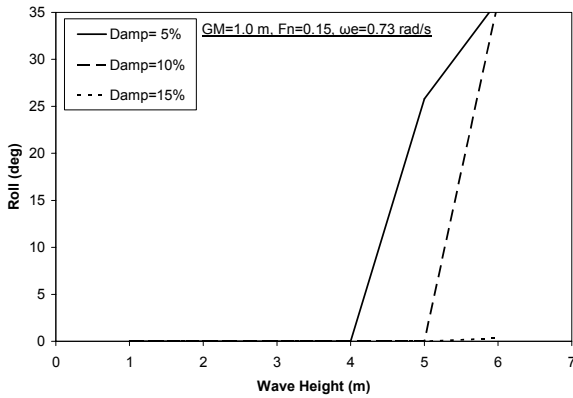


Figure 11 Roll vs. wave height for RoRo ship at GM=1.00m and Fn=0.15

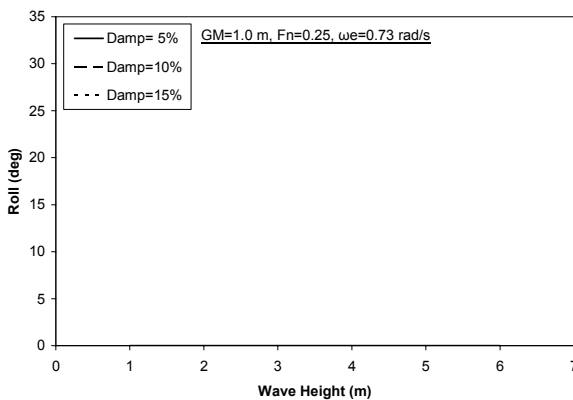


Figure 12 Roll vs. wave height for RoRo ship at GM=1.00m and Fn=0.25

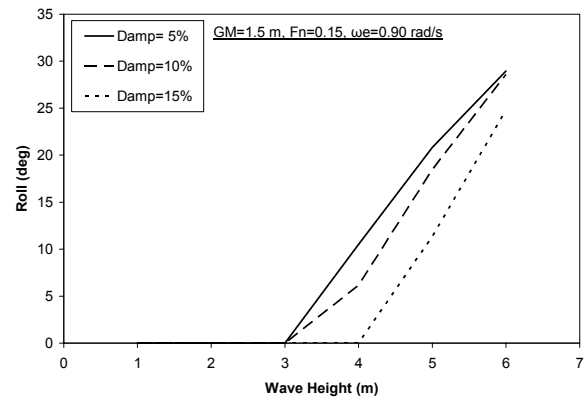


Figure 13 Roll vs. wave height for RoRo ship at GM=1.50m and Fn=0.15

The roll viscous damping seems to shift the occurrence of the roll resonance towards the higher wave amplitudes. Furthermore, the increase of roll stiffness (GM=1.50m) seems to favors resonance.

The tested range of wave heights for the RoRo ship practically corresponds to the left-side range of the numerical tests for the fishing vessels. The occurrence of resonance at a certain wave height and the increase of roll amplitude thereafter appear to be common features of both vessels.

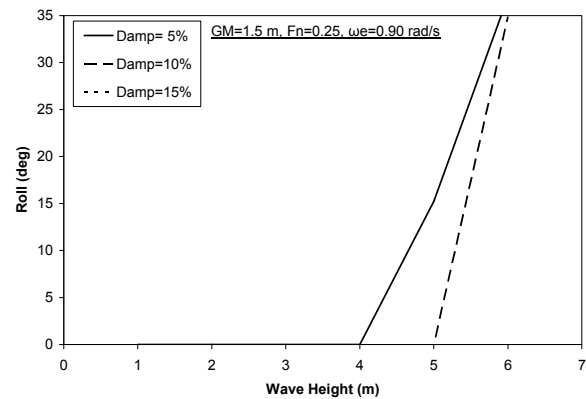


Figure 14 Roll vs. wave height for RoRo ship at GM=1.50m and Fn=0.25

5. DISCUSSION OF RESULTS

The roll resonance observed in the undertaken numerical tests for two different types of vessels is a typical head seas parametric roll resonance phenomenon. The

roll amplitude amplification is a direct consequence of the parametric variation of ship's restoring characteristics in view of the wave induced ship motions.

A detailed analysis of the motion and the forces has shown that, as GM is a non-linear function of the induced pitch motion as the ship advances in head waves, it varies in time inducing a periodic change of the restoring moments at a frequency equal the wave encounter frequency.

In Figure 15 and Figure 16 below, the metacentric height GM is depicted as function of trim (correspondingly pitch) for the fishing and RoRo vessel respectively, as calculated for the calm water conditions. These diagrams show the strong dependence of GM on the trim (pitch) and illustrate the expected variation of GM when pitch oscillates, at least for the hydrostatic term.

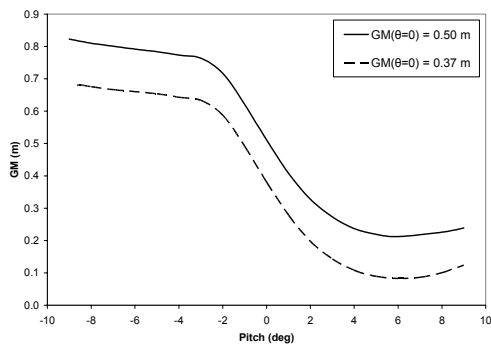


Figure 15 GM as function of pitch for the fishing vessel

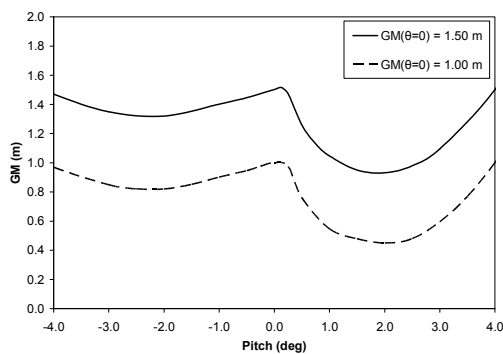


Figure 16 GM as function of pitch for the RoRo vessel

Figure 17 shows how the GM effectively changes in time in the presence of waves for the conditions corresponding to Figure 4. This GM differs to the one depicted in above figures, as it includes also hydrodynamic effects, namely it is the tangent of the actual restoring roll moment at the zero angle of heeling.

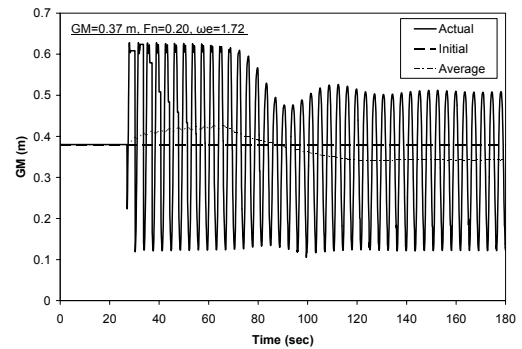


Figure 17 GM variation in time for the fishing vessel

It can be seen that the time averaged GM value remains quite constant at the beginning of the simulation where no roll motion occurs, namely it is equal to the hydrostatic value $GM = 0.37$ m, here denoted as initial GM. However, as vessel starts rolling the averaged GM changes and reaches in the steady state condition, after about 120 seconds, a value of about 0.33 m.

Similarly, in Figure 18 the GM variation is sampled for the steady state response of the RoRo ship where the roll amplitude has reached a value of 15 degrees after time 500 sec.

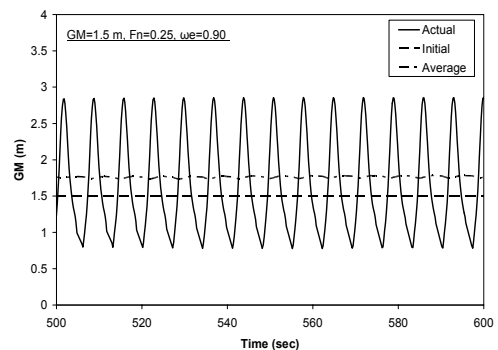


Figure 18 GM variation in time for the RoRo ship

In this case the average GM in the steady state response seems to be higher than the initial GM value. The observed changes of the average GM under the dynamic wave-induced conditions allow us the introduction of the notion of *effective GM in waves*, which is different to the initial GM in calm water.

Insight to the roll motion excitation mechanism is obtained by reviewing the hydrostatic GZ variation during a roll period, as illustrated with the Figure 19. In this diagram the righting arm GZ curves of constant pitch (trim) are plotted together with the actual hydrostatic GZ during a numerical test. The shape of the actual GZ-heel correlation is a symmetrical double-loop knot. The vessel while heeling from the upright position has a low GM value, which corresponds to the curve of constant pitch $\theta = +2.0$ deg (trim by bow). Then, as the vessel has heeled about +2 degrees it gradually changes its pitch to $\theta = -2.0$ deg (trim by stern) with a consequent increase of GZ and hence of the restoring moment. The vessel reaches its maximum heeling angle and then returns to the upright position under the excitation of higher restoring moment. This loop is repeated to the opposite side.

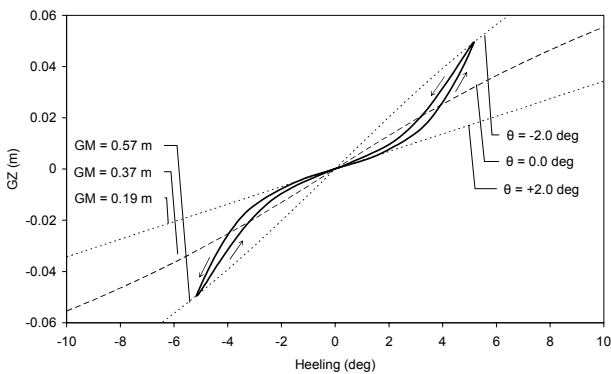


Figure 19 GZ variation in parametric rolling

Consequently the pitch motion, as a result of the wave excitation, changes the underwater part of the hull and subsequently the restoring moment, which in turn controls the roll motion. Hence, the coupling between roll and pitch motion is obviously a determinant factor for

the occurrence of the roll resonance in head waves.

The discussion on the background mechanism of the observed roll motion is herein complemented by an elaboration regarding finiteness of the roll amplitude recorded in roll resonance. For this purpose the diagram of Figure 20 is presented, where the roll amplitude is depicted for constant wave amplitudes and varying wave encounter frequency. Three response curves for different wave amplitudes are plotted. The double of the natural frequency is indicated with a vertical dashed line.

These results suggest the occurrence of a nonlinear roll resonance, similar to that depicted in the explanatory schematic Figure 21. The response curve is bended towards the lower frequencies indicating a jump phenomenon marked with dotted lines. The bending towards the lower frequencies is a direct consequence of the non-linear stiffness for the roll motion. It is specifically due to the convex character of the GZ curve versus roll angle.

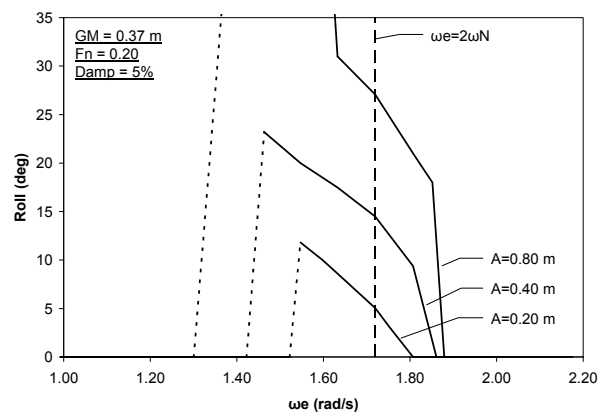


Figure 20 Non-linear roll resonance for the fishing vessel

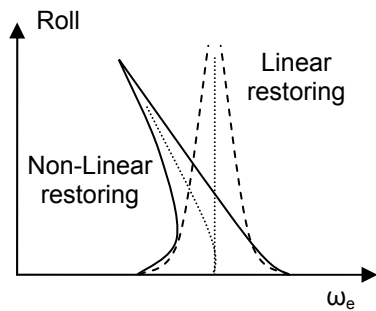


Figure 21 Basic behavior of roll resonance with linear and non-linear restoring

The presence of such non-linearity is the cause of the finiteness of the roll amplitude in parametric roll for the studied frequency ($\omega_e = 2 \omega_N$). In parametric resonance with linear restoring the amplitude would grow exponentially to infinity. The consideration of non-linear effects results to a saturation of the roll growth and thus finite roll amplitudes are recorded.

The roll amplification observed in Figure 20 occurs over a finite range of frequencies of considerable width. In case of irregular wave excitation, a strong interaction with the wave components around the double roll natural frequency can be expected, particularly if the wave energy density is high in the amplification bandwidth.

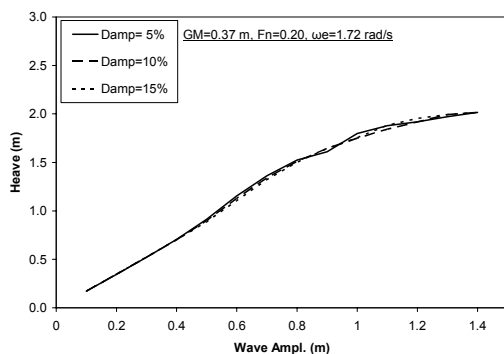


Figure 22 Heave response amplitudes for the fishing vessel

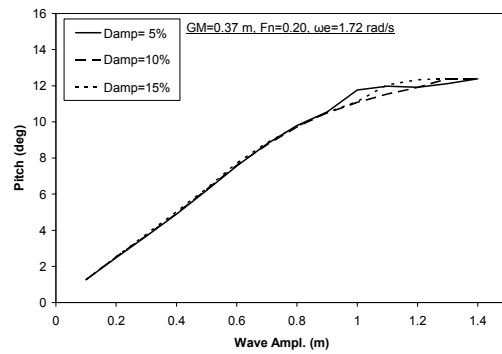


Figure 23 Pitch response amplitudes for the fishing vessel

While the roll motion strongly depends on the incoming wave amplitude, the other two motions, that of heave and pitch, are less affected by non-linear effects of wave amplitude, as demonstrated in Figure 22 and Figure 23 for the fishing vessel. Note that in case of the RoRo ship, these functions remain practically linear in the studied range of waves as demonstrated in Figure 24 for the pitch motion.

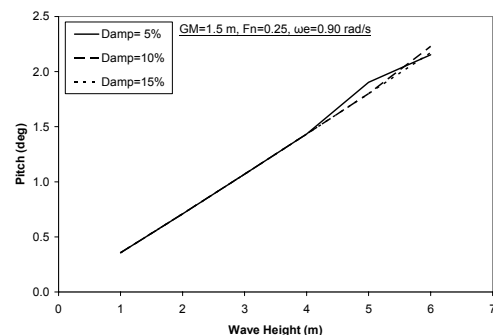


Figure 24 Pitch response amplitudes for the RoRo ship

6. CONCLUSIONS

The motion of two different types of vessels, namely a fishing boat and a RoRo ship, in parametric roll conditions in regular head waves has been studied with use of a nonlinear 6 DOF time domain numerical simulation method. The simulated results and subsequent analysis provide insight and improved understanding of the parametric roll resonance mechanism. Both vessels respond quite

likewise despite the fundamental differences of their hull forms.

The presented work revealed several aspects of the time domain simulation method, which are quite valuable for the validation of the method prior to its application for the assessment of the probability of the parametric roll in actual sea waves.

It proved that the non-linear character of the restoring moment and the coupling of the roll-pitch motion are the determinant factors for the induced roll resonance at wave encounter frequency close to the double roll natural frequency.

In terms of stability, it has been observed that capsizes due to intensive parametric roll can occur in presence of considerable wave amplitudes combined with low roll damping characteristics.

Findings at the range of even larger wave amplitude excitation, where the induced roll amplitude seems to decrease (and even completely diminish) with the increase of the wave amplitude, need further investigation in order to explain the observed phenomenon, identified also in relevant physical model experiments.

7. ACKNOWLEDGEMENTS

The present study was partly supported by the European Commission under the FP6 Sustainable Surface Transport Programme, namely the Integrated project SAFEDOR (Design, Operation and Regulation for Safety, task 2.3) Contract No. FP6-IP-516278 and the STREP project ADOPT (Advanced Decision Support System for Ship Design, Operation and Training), Contract No. FP6-TST4-CT-2005-516359. The European Community and the authors shall not in any way be liable or responsible for the use of any such knowledge, information or data, or of the consequences thereof.

8. REFERENCES

- Belenky, V.L., Weems, K.M., Lin, W.M., Paulling, J.R., 2003. "Probabilistic Analysis of Roll Parametric Resonance in Head Seas." Proc. of 8th Inter. Conf. on Stability of Ships and Ocean Vehicles, STAB2003, Madrid, Spain, pp.325-340.
- Cummins, W., 1962. "The impulse response function and ship motions," Journal Schiffstechnik, Vol. 9, no. 47, pp. 101-109, June
- France, W.M., Levadou, M., Treakle, T.W., Paulling, J.R., Michel, K. and Moore, C. 2003. "An Investigation of Head-Sea Parametric Rolling and its Influence on Container Lashing Systems", Marine Technology, Vol. 40, No. 1, pp 1-19.
- Francescutto, A., Bulian G., 2002. "Nonlinear and Stochastic Aspects of Parametric Rolling Modeling", Proceedings of International Ship Stability Workshop, Webb Institute, USA.
- Hashimoto, H., Matsuda, A., Umeda, N., 2005. "Model Experiment on Parametric Roll of a Post-Panamax Container Ship in Short-Crested Irregular Seas", Conference Proceedings of the Japan society of naval architects and Ocean Engineers, vol.1, pp.71-74, Nov. 2005
- ITTC, The specialist committee on Stability in Waves, 2005. "Final report and recommendations to the 24th ITTC"
- Krueger S., Kluwe, F., 2006. "Development of Dynamic Stability Criteria from Direct Seakeeping Simulations". Proc. of the 9th Inter. Marine Design Conference, Ann Arbor, MI, USA.
- Lee, H.-H., Lee I.-H., Lee Y.-W., Yoon, M.-T., 2006. "Experimental and Numerical Investigation into the Parametric Roll Resonance in Head Seas for an Ultra Large Containership", Proceedings of the 9th Inter. Marine Design Conference, Ann Arbor, MI, USA.

-
- Neves, M. A. S., Rodriguez, C.A., 2005. "Stability Analysis of Ship Undergoing Strong Roll Amplifications in Head Seas". Proceedings of the 8th International Ship Stability Workshop, Istanbul Technical University, Istanbul, Turkey.
- Neves, M., Perez, N., Lorca, O., 2002. "Experimental Analysis on Parametric Resonance for Two Fishing Vessels in Head Seas", Proceedings of the 6th International Ship Stability Workshop, Webb Institute, NY, USA
- Papanikolaou, A., 1989. "NEWDRIFT V.6: The six DOF three-dimensional diffraction theory program of NTUA-SDL for the calculation of motions and loads of arbitrarily shaped 3D bodies in regular waves", Internal Report, National Technical University of Athens, NTUA-SDL
- Ribeiro e Silva S., Santos T.A., Soares G., 2005. "Parametrically Excited Roll in Regular and Irregular Head Seas". Int. Shipbuilding Progress, Vol. 52, no. 1, pp.29-56.
- Spanos, D., 2002. "Time Domain Simulation of Motion and Flooding of Damaged Ships in Waves", Doctoral Thesis, Ship Design Laboratory, National Technical University of Athens
- Spanos, D., Papanikolaou, A., 2005." Numerical Simulation of a Fishing Vessel in Parametric Roll in Head Seas", Proc. of 8th Inter. Workshop on Stability and Operational Safety of Ships, Istanbul, Turkey, October 6-7, 2005
- Spanos, D., Papanikolaou, A., 2005b. "Yaw drift moment of a floating structure in waves, Proceedings of 24th Inter. conf. on Offshore Mechanics & Arctic Engineering", OMAE05, June 12-17, 2005, Halkidiki, Greece.
- Umeda, N., Hashimoto, H., Vassalos, D., Urano, S., Okou, K., 2003. "Nonlinear Dynamics on Parametric Roll Resonance with Realistic Numerical Modelling", Proc. of 8th Inter. Conference on the Stability of Ships and Ocean Vehicles STAB03, University of Madrid, Spain